

Research Article

Metallographic Investigation on Postweld Heat-Treated 0.21%C-1020 Steel Plates Joined by SMAW Method

Saurabh Dewangan ¹, Senthil Kumaran Selvaraj ², Karthikeyan B ³,
Tezeta Moges Adane ⁴, Somnath Chattopadhyaya ⁵, Grzegorz Królczyk ⁶,
and Ramesh Raju ⁷

¹Department of Mechanical Engineering, Manipal University Jaipur, Jaipur, Rajasthan 303007, India

²Department of Manufacturing Engineering, School of Mechanical Engineering (SMEC), Vellore Institute of Technology (VIT), Vellore-632014, Tamil Nadu, India

³School of Civil Engineering, SASTRA Deemed to be University, Thanjavur 613401, India

⁴School of Civil Engineering, Engineering and Technology College, Dilla University, P.O. Box 419, Dilla, Ethiopia

⁵Department of Mechanical Engineering, Indian Institute of Technology (ISM), Dhanbad, Jharkhand 826004, India

⁶Faculty of Mechanical Engineering, Opole University of Technology, ul. Mikolajczyka 5, 45-271, Opole, Poland

⁷Department of Mechanical Engineering, Sree Vidyanikethan Engineering College (Autonomous), Tirupathi 517102, Andhrapradesh, India

Correspondence should be addressed to Senthil Kumaran Selvaraj; senthilkumaran.s@vit.ac.in

Received 8 August 2022; Accepted 17 September 2022; Published 12 October 2022

Academic Editor: Sonar Tushar

Copyright © 2022 Saurabh Dewangan et al. This is an open access article distributed under the Creative Commons Attribution License, which permits unrestricted use, distribution, and reproduction in any medium, provided the original work is properly cited.

This paper presents analysis and comparison into mechanical behaviour and microstructural attributes of postweld heat-treated AISI 1020 (0.21%-C) plates joined by the shielded metal arc welding (SMAW) process. The purpose of this work is to heat the welded samples uniformly so that a possible formation of austenite can be obtained, and hence, residual stresses, if any, can be recovered. Four pairs of such steel were taken and welded to form four joints. Welding was followed by heat treatment. The heating temperature and holding time were selected as 1040°C and 60 minutes, respectively. Different cooling media such as sand, water, oil, and air were used to cool the samples. Hence, there were four different samples according to their physical conditions: sand-cooled, water-quenched, oil-quenched, and air-cooled. For analysing mechanical behaviour of all the plates, standard-shaped specimens were prepared out of them. The tensile strength, impact strength, hardness, and the microstructural attributes were analysed in four welded samples after heat treatment. Significant variations in tensile strength and hardness were reported when compared with each other. Oil-cooled sample showed a remarkable enhancement in tensile strength. The sand-cooled sample possessed the highest toughness, whereas water-quenched samples were found to be highly hard. Furthermore, a good combination of strength, hardness, and ductility was reported in oil-cooled sample. Pearlite (coarse and fine) and martensite were the main microstructural findings in the study. A clear vision of ferrite, cementite, and martensite on various heat-treated samples made this study important. All the mechanical properties are in good corroboration with microstructure. A significant refinement into all the mechanical properties was achieved in this work.

1. Introduction

Steel is one of the highly demanded metals all over the world. Different grades of steels are used for different working conditions. In such grades, AISI 1020 is very common and is

extensively used for construction, fabrication, and manufacturing of different products such as angle, channel, bars, slabs, and sheets. AISI 1020 steel possesses an ideal combination of formability, weldability, and machinability [1–3]. This grade comes under low carbon steel category.

Hence, the carbon content varies between 0.1 and 0.2%. Some important properties and ingredients of 1020 steel are written in Tables 1 and 2. The most important characteristic of the steel is to change the mechanical properties according to various heating and cooling methods. Heat treatment can reform the properties of the metal as per the requirement. In addition, the annealing heat treatment technique is adopted to remove the internal stresses in the steel specially in welded joint. The fusion welding process imparts a complex cooling and solidification phenomena. As the welded zone is suddenly converted into liquid state, a lot of thermal gradients is produced on the other parts of the welded plate [5]. Therefore, there is always a chance of formation of residual stresses in the heat-affected zone and welded zone. Other defects such as strain hardening due to improper cooling can also be generated in the welded joint. These defects begin to remove as soon as recrystallization starts in the γ -austenite zone [6].

Analysis of postweld heat-treated plates is not a new development. This research work has been taken into consideration by many researchers in the last two decades. Still, in the view of production economy and wide application of the steel, continuous research is necessary. Here, some of the previous research works are summarized as follows.

PWHT is conducted to achieve stability in metallurgical structure and to increase service life of the steel [7]. After applying PWHT, Yamaguchi et al. [8] noticed that the heat-affected zone (with fine-grained structure) possessed higher fatigue strength than that of fusion line and weld metal zone. Jorge et al. [9] conducted multipass welding of HSLA-80 steel by using a coated electrode. They used five different conditions: only preheating, pre and postheating, only postheating, and without pre- or postheating. They concluded that there was a minor influence of heat treatment on the welding of this steel. The toughness was reported high at the heat-affected zone of heat-treated samples.

In an experiment, H13 hot worked tool steel was heat-treated in three different conditions, i.e., (a) after tempering; (b) while quenching; and (c) while tempering. High hardness was reported on the tool steel after applying heat treatment methods. Steel was found to be hardened due to the presence of retained austenite [10]. The pretempering treatment was applied on two different kinds of steels, i.e., quenched and partitioned steels. These steels possessed ferrite and martensite structures. During experiment, both microstructure and mechanical properties of the steel got affected. The treatment had increased the strength and toughness of the samples [11]. In a work, the high strength steel (with Fe, C, and Mn as main constituents) was tempered. As a result, cementite got coarser. Due to this, Mn was found to get partitioned from the cementite matrix [12]. The restoration and recovery of retained austenite (intermixed with martensite) were done by applying the thermo-mechanical technique. As a result of thermal recovery, degree of dislocation got reduced, and therefore, martensite got softened [13]. A high chromium cast iron was tempered to check the microstructural and mechanical property variation. As a result of tempering, hardness got reduced, and the material

became more tough and highly wear-resistant [14]. Calik [15] investigated the hardness variation in relation with microstructure by adopting various cooling rates in steels. As soon as the cooling rate was enhanced, the hardness got increased. Accordingly, the microstructure had also changed significantly. Htun et al. [16] found that, as soon as the tempering time and temperature were increased, the hardness and ultimate tensile strength got reduced. Machado [17] conducted heat treatment of two different grades of steels, i.e., AISI 1020 and 52100 with an application of electrical power. The effect of input voltage on hardness was observed. Hardness was greatly enhanced by increasing voltage input.

In the direction of improvement of mechanical properties, the present work deals with postweld heat treatment of low carbon steel (1020 grade). As the manual welding of the steel plates was done through SMAW, there might be chances of nonuniform cooling of welded zone up to room temperature by Kumaran et al. [18–20]. In such cases, the solidified welded joint may contain residual stresses which is the main cause of joint failure in impact loading condition. In general, the predominant effects of residual stresses remain at the heat-affected zone as it is the zone which does not melt but undergoes some microstructural variations due to high temperature. To remove any residual stresses or irregularity (if present) in microstructure of as-welded plate, heat treatment was performed. Such heat-treated samples were compared with each other based on the mechanical properties and microstructural attributes.

2. Materials and Methods

The experimental work imparts shielded metal arc welding of four pairs of AISI 1020 (0.21% C) steel plates. Each plate has a dimension of $100 \times 50 \times 5$ mm. A proper edge preparation was done prior to welding. The voltage and current, i.e., 65 V and 150 A were selected for welding the plates. Hence, the ideal heat input ($P = V \times I$) was 9750 J/s. With this high heat input, a common welding speed of 5 mm/s was selected for each pair of welding. The cellulosic electrode of grade E6010 containing low carbon steel rod with 2.5 mm diameter was used as electrode material. The yield parameters for welding were randomly selected as our main aim was to find the effect of heat treatment on mechanical properties and microstructure behavior. After welding and cooling of all the plates, heat treatment methods were followed. For this purpose, all the plates were heated in furnace. The heating time was common for all the samples which is 60 minutes. For that period, the temperature was maintained at 1040°C. Temperature measurement was done by means of a laser pyrometer. The heated samples were, then, taken out one by one. First sample (sample A) was put inside the sand for cooling up to room temperature. The sand is the same which is used for construction purpose. Second sample (sample B) was dipped into 1 l water to cool down at room temperature. Water took least time to cool down the heated plate. Third plate (sample C) was dipped into 1 l oil for cooling purpose. Mustered oil was used for this work. Fourth sample (sample D) was taken out from the furnace and kept

TABLE 1: Physical properties of 1020 (0.21%-C) steel [3].

Properties	Ultimate tensile strength	Yield strength (MPa)	Elongation (%)	Hardness (BHN)	Impact energy (J)
Values	≈600 MPa	362	25	224	101

TABLE 2: Elements included (approximately in weight %) in 1020 steel [4].

Sr. no.	Elements	Composition by weight, %
1	Carbon	0.210%
2	Silicon	0.25%
3	Manganese	0.83%
4	Nickel	0.085%
5	Chromium	0.08%
6	Molybdenum	0.02%
7	Phosphorous	0.006%
8	Iron	Rest

in open atmosphere to allow it for cooling in air. It was noticed that sand cooling took the longest time, whereas water cooling time was too small. A welded plate and open-hearth furnace are shown in Figure 1. From every heat-treated sample, tensile test specimen was prepared according to the ASTM E-8 M standard [21]. For this purpose, wire-EDM was used to cut the steel samples (as shown in Figure 1). The tensile test specimens are shown in Figure 2. Brinell hardness test was conducted to find variation in hardness from the welded zone to base metal zone. The load was taken as 1500 N for conducting hardness test. One sample from every welded plate was cut and polished at its cross-sectional area. The polished surface underwent microexamination to detect possible changes in grain structure after heat treatment.

3. Results and Discussion

After performing experiments and tests, all the results were noted down properly. This section includes a complete detail of parameters selected for experiments, procedure of tests, and detailed findings of work. The result analysis and discussion are as follows.

3.1. Mechanical Behavior

3.1.1. Tensile Test. All the welded and heat-treated plates underwent through two different mechanical tests, i.e., tensile test and hardness test. The tensile test was performed on FIE Make Universal Testing Machine (UTM), UTES-100. The tensile specimens were prepared according to ASTM E-8 M standard in which the gauge length was kept as 45 mm. The rate of deformation was selected as 0.0001/s. The stress-strain graphs of four specimens are shown in Figure 3. For each test, the corresponding values of tensile strength, maximum force, and elongation are shown in Table 3.

It can be noticed that the nature of curves is similar in sample A (sand-cooled) and sample D (air-cooled). Also, there is much similarity in the oil-cooled and water-cooled samples. Sample D has a tensile stress value of 200 MPa and a good extension of 0.7 mm. Higher strain value indicates the

lower value of modulus of elasticity (stress/strain). The modulus of elasticity in the air-cooled sample was reported as 57551 MPa. The similar kind of characteristics were observed in sand-cooled specimen but with improved material properties. The tensile stress value of 332 MPa was found in sand-cooled sample. This value is almost 66% greater than air-cooled sample. The load requirement to achieve this tensile strength is 11960 N. It is the highest value of load as compared to other samples. Also, the extension of the sample A (sand-cooled) at the tensile strength is 1 mm. It is the maximum extension among all the samples. It indicates that the sand-cooling method has increased the ductility of the sample.

Sample B (water-cooled) has shown the tensile stress of 289 MPa which is 44% higher than air-cooled sample and 13% lower than sand-cooled sample. Hence, the water-cooling process has drastically increased the tensile stress as compared with the air-cooled sample. The extension at tensile strength is 0.2 mm which is much lesser than the same of sand- and air-cooled samples. Therefore, water cooling has reduced the ductile behavior of the sample. As the sample has showed less value of strain, it possesses the highest value of modulus of elasticity, i.e., 69399 MPa among all samples. The oil-cooled sample, sample C, has shown almost similar characteristics as those of water-cooled sample. However, the tensile stress (550 MPa) is almost 90% higher as compared with sample B. Also, there is an increment of 146% was observed in extension value in comparison with sample B. The possible reason of the highest tensile strength in oil-quenched sample is the formation of a mixture of martensite and very fine pearlite (i.e., bainite). Bainite structure provides a good strength to the steel. A comparative assessment between water-quenched and oil-quenched samples are shown in Figure 4.

3.1.2. Fractographic Test. The middle part of broken tensile specimens was observed under field emission scanning electron microscopy (FESEM) for observing the fracture behavior of the specimens. All the specimens got broken through welded joint but with different fracture behavior. Figure 5 shows the fractographic images of all the samples. Figure 5(a) belongs to water-quenched specimen. As per an approximate observation, it has low magnitude of peaks and valleys which is an indication of brittle fracture. Also, cracks and cleavage facet [22] were significantly available in the sample as an indication of brittle fracture, although many dimples are also visible in the sample as a sign of ductile failure. Unlike water-quenched sample, oil-quenched specimen is not possessing facets and cracks. Also, the peaks and valleys formation are high enough to prove a ductile fracture of the specimen. In addition, there are many microdimples available in the fractured zone (Figure 5(b)). Figure 5(c) is an image of sand-cooled specimen with full of



FIGURE 1: Experimental procedure. (a) Welded plates were heated in an open-hearth furnace; (b) temperature values were observed by using a pyrometer; (c) sample preparation for further analysis; (d) a tensile test specimen prepared by using wire-EDM.

dimples and significant magnitude of peak (shown inside a rectangular area) and valley (shown inside a circular area). No cracks are visible on the fracture zone. Therefore, it is clear indication of ductile fracture. In Figure 5(d), the air-cooled specimen is possessing lesser amount peaks/valley than sand-cooled sample. Some cracks and facets are available, but they are in lesser quantity than in water-quenched sample. A lot of dimples are present throughout the area. It shows a combination of both brittle (in a little magnitude) fracture and ductile fracture.

3.1.3. Hardness Test. The hardness of the welded zone, heat-affected zone, and base metal zone was analysed by the Brinell hardness tester. The steel ball indenter was used for this purpose. Hardness test was performed at a load of 1500 N. Prior to conducting the test, one side of the cross-sectional surface of each plate was smoothed properly so that a good result could come out. The center point of the welded zone is marked as "0." Besides center point, there were eight indents were made on either side of the plate. Just for reference purpose, negative sign was used for leftward

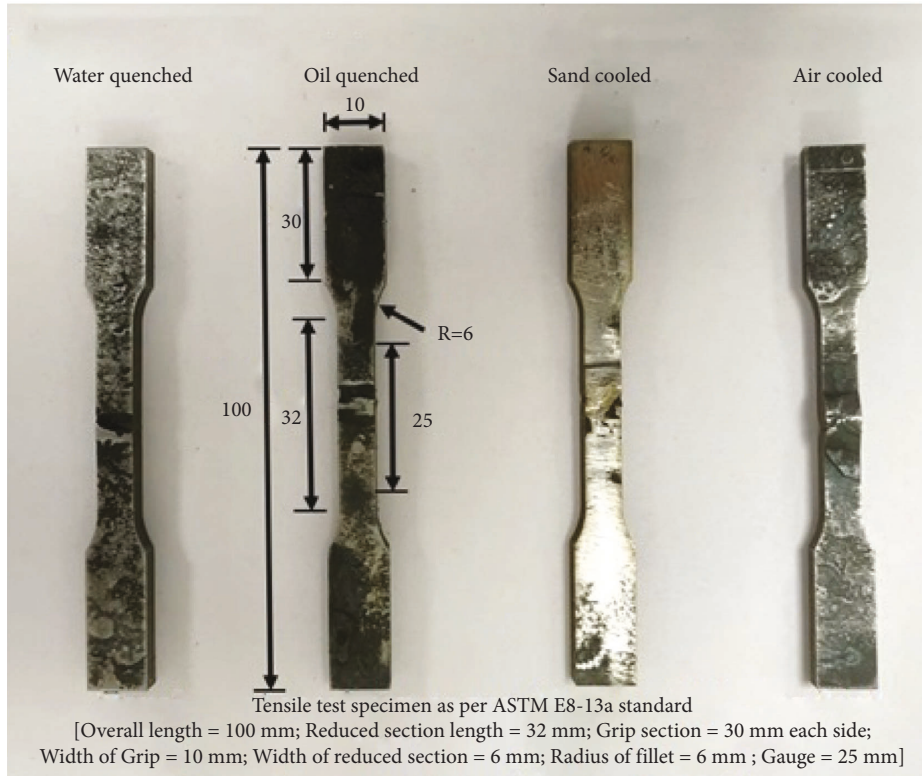


FIGURE 2: Tensile test specimens as per ASTM E-8 M standard.

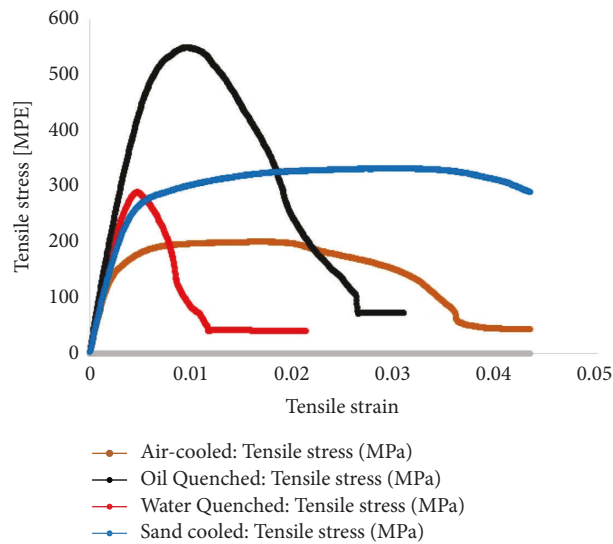


FIGURE 3: Tensile test and stress-strain diagrams of (a) sand-cooled; (b) water-cooled; (c) oil-cooled; and (d) air-cooled samples.

indents and positive sign was used for rightward indents. An appropriate gap between two consecutive indents was maintained so that the plastic deformation zone of the previous indent could not affect the next indent area. By using graph, hardness profile of each sample is compared as shown in Figure 6. Representation of indentation on the cross-sectional surface is shown in Figure 6. Hardness profile of all the samples is similar. A common observation with all

the samples is that the welded zone possesses higher hardness than other parts.

3.1.4. Impact-Energy Test. The Charpy test was used to analyze the impact energy of the welded joints. The samples were prepared as per the testing requirement. “V” notch was cut from the weld centreline in such a way that a common

TABLE 3: Different parameters corresponding to tensile test.

Properties/ Specimen	Air-cooled	Water-quenched	Oil-quenched	Sand-cooled
Tensile strength (MPa)	200	289	550 (175%↑ than air-cooled; 90%↑ than water-quenched; 66%↑ than sand-cooled)	332
Extension at tensile strength (mm)	0.7	0.2	0.5	1 (43%↑ than air-cooled; 400%↑ than water-quenched; 100%↑ than oil-quenched)
Load at tensile strength (N)	7214	10424	9013	11960 (66%↑ than air-cooled; 15%↑ than water-quenched; 33%↑ than oil-quenched)
Modulus of elasticity (MPa)	57551	69399 (20%↑ than air-cooled; 13%↑ than oil-quenched; 22%↑ than sand-cooled)	61344	57024

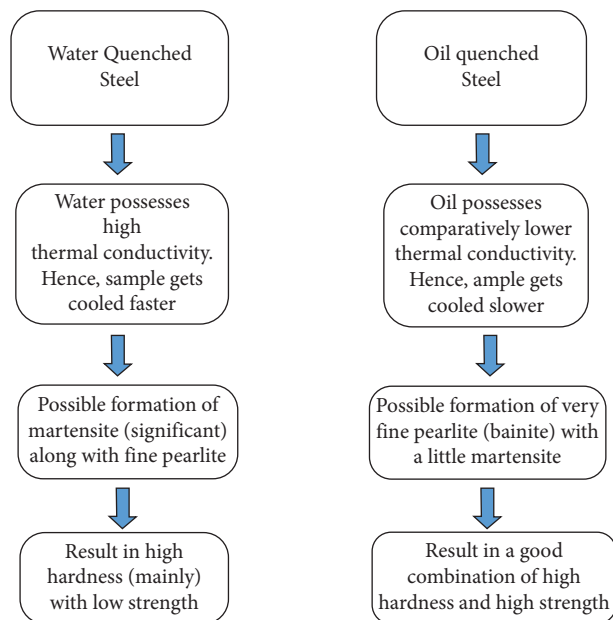


FIGURE 4: Comparative assessment between water-quenched and oil-quenched samples.

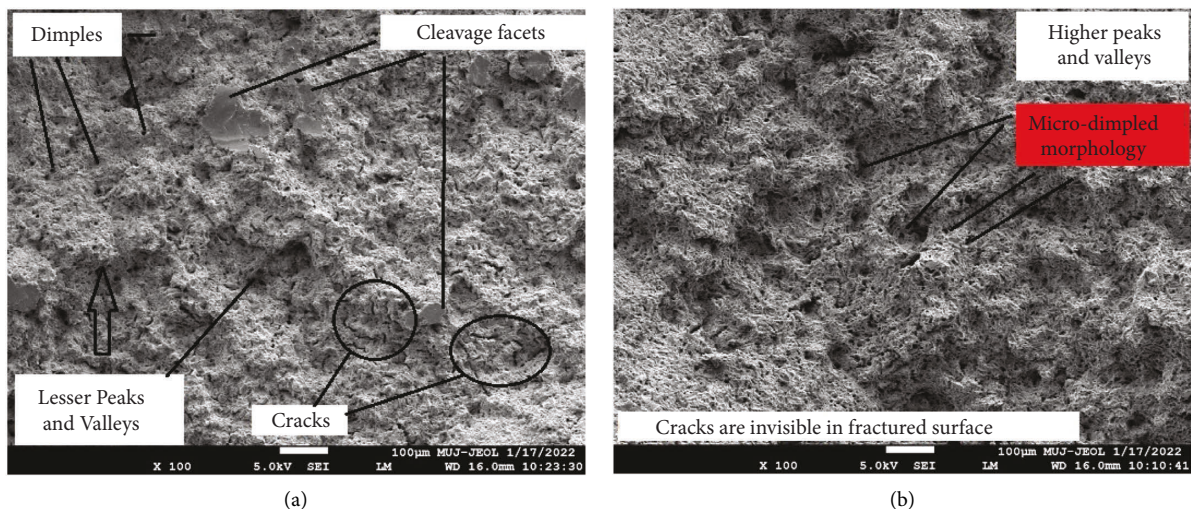


FIGURE 5: Continued.

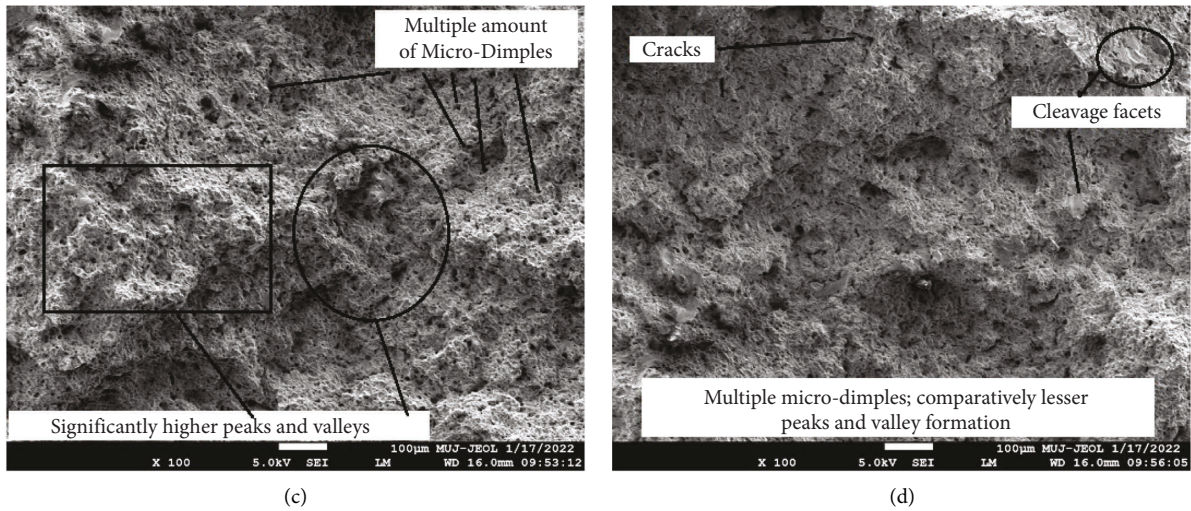


FIGURE 5: Fractographic analysis of specimens broken through tensile test. Observation into (a) water-quenched specimen, (b) oil-quenched specimen, (c) sand-cooled specimen, and (d) air-cooled specimen.

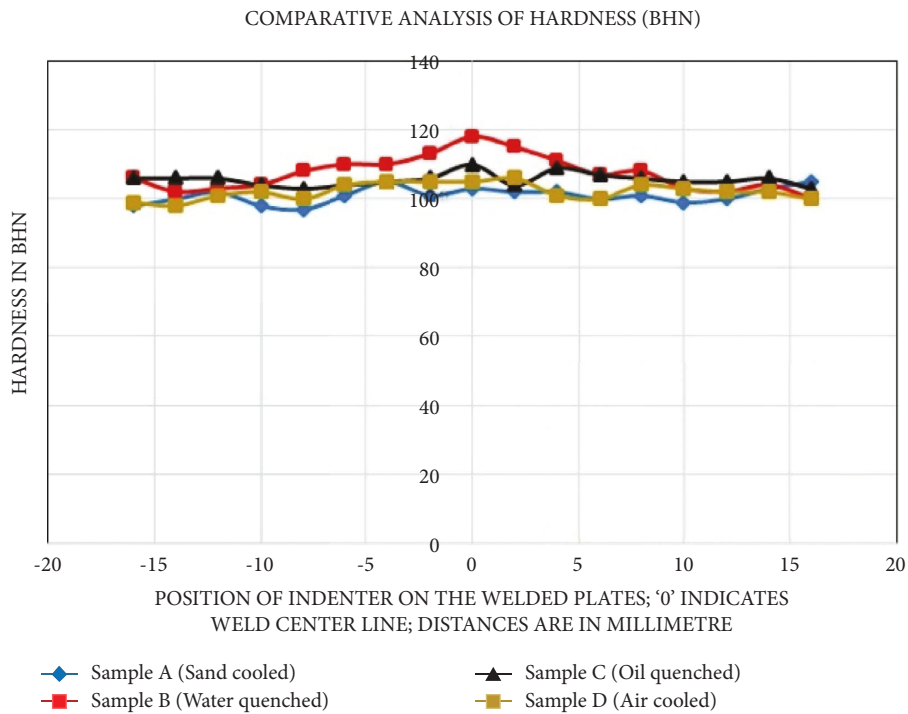


FIGURE 6: Hardness profile of all the samples; the welded zone possesses high hardness.

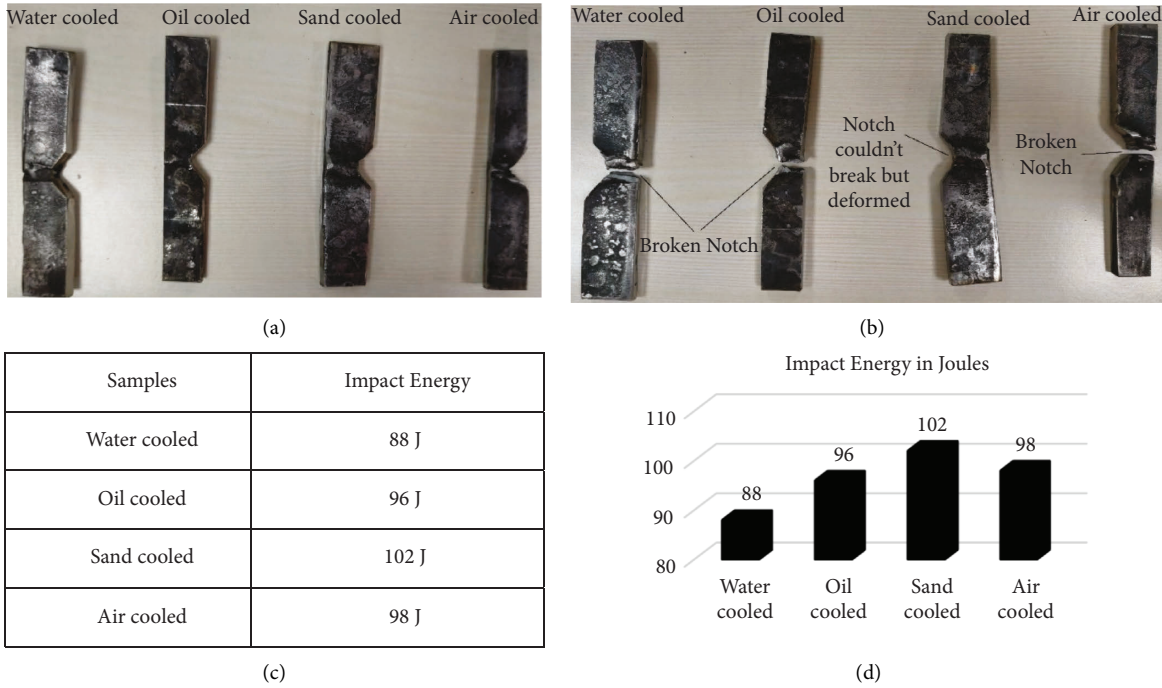


FIGURE 7: (a) Specimens of impact strength analysis. (b) Broken samples after test. (c) Values of impact strength. (d) A comparative analysis among all samples.

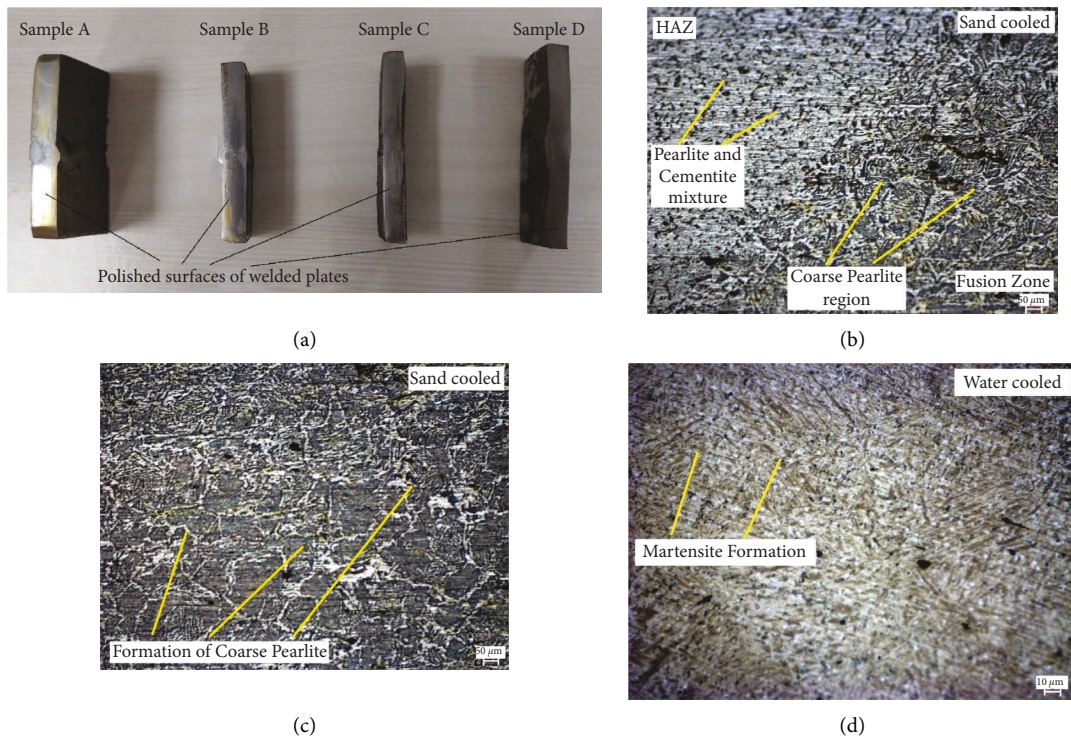


FIGURE 8: Continued.

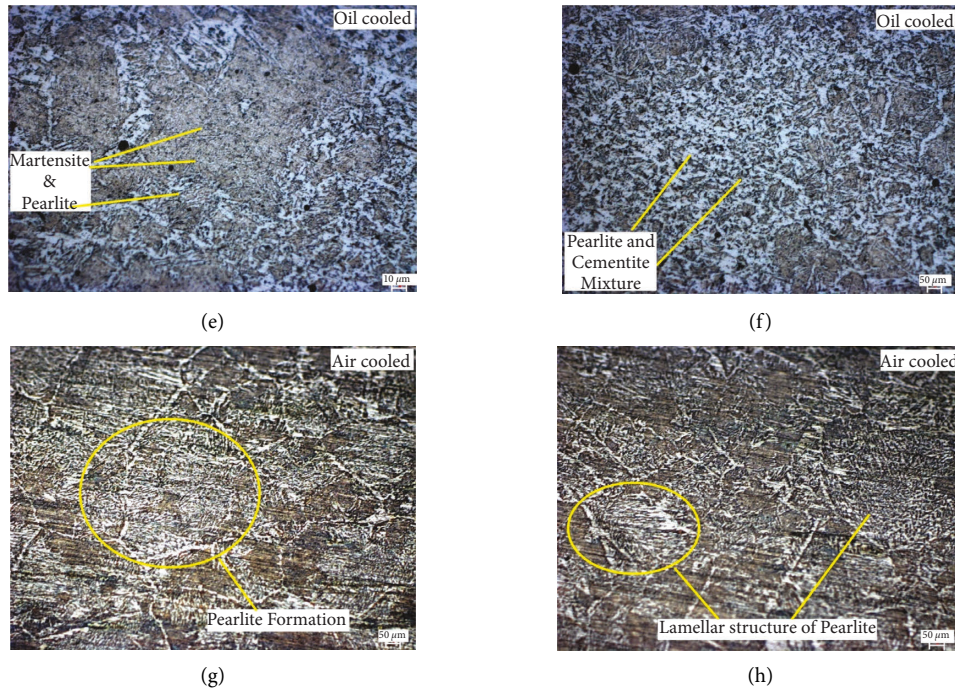


FIGURE 8: Polished welded plates and microstructures. (a, b) sand-cooled samples with coarse pearlite; (c) water-cooled sample with martensite formation; (d, e) oil-cooled sample possesses both pearlite and martensite as well as cementite-mix region; (f, g) air-cooled sample with lamellar structure of pearlite regions.

angle of 110° can be formed, as shown in Figure 7(a). A hammer, set at an inclination of 135° from the actual position of the specimen, was allowed to fall freely through the specimens. As soon as hammer breaks the samples through its notch, the value of impact energy is shown by the energy indicator. The values of impact energy for each specimen are shown in Figure 7(c). The broken/deformed samples are shown in Figure 7(b). Also, a comparative analysis among the toughness of the samples is also shown by a bar chart in Figure 7(d). It was noticed that all the samples were broken in this test except sand-cooled sample. The impact energy consumed by sand-cooled sample was found the highest, i.e., 102 J among all. On the other side, water-cooled sample showed the least value of impact strength, i.e., 88 J. The impact test results are as per the expectation drawn after observing fractographic images.

3.2. Microstructural Behavior. For microstructural observation, the samples were properly polished with abrasive papers of grit sizes 1000, 1500, and 2000. *Nital* reagent was used as an etchant with 2.5% nitric acid and 97.5% ethanol. By using a thick cotton, the etchant was fully spread on the highly polished surface of the welded plate for nearly 1 min. The polished samples and microstructural images captured for each sample are shown in Figure 8.

Figures 8(a) and 8(b) show the microstructural images of sand-cooled sample. In this, a clear view of coarse pearlite and cementite is available. In the fusion zone, the coarse pearlite in lamellar form is visible. In addition, there is a difference in microscopic view of heat-affected zone and

welded zone. As sand provides slow cooling rate, the gamma-austenite got a sufficient time to fully convert into coarse pearlite. As the previous study reveals, the coarse pearlite makes the steel ductile and tough [3]. In this work, sand-cooled specimen was reported comparatively more ductile due to possessing coarse pearlite. Figure 8(c) shows the microstructure of water-cooled sample. This image has completely different appearance than Figures 8(a) and 8(b). The acicular martensite was observed in the water-cooled sample. As water cooling occurs at very fast rate, austenite does not convert into 100% pearlite. Some amount of retained austenite is remained with pearlite. Therefore, this needle-like structure makes the sample very hard. It can be corroborated with hardness test also. The water-cooled sample possessed the highest hardness among all samples.

Figures 8(d) and 8(e) are referred to microstructures of oil-cooled sample. In these images, there were three different structures observed. The bright-coloured zones are ferrites which are surrounded by dark zones, cementite. Cementite possesses dark appearance due to carbon composition in it. Specifically, in Figure 8(d), the martensite was found to be surrounded by pearlite (ferrite + cementite). This martensite is nothing but retained austenite resulted by the rapid cooling process. Although this sample possesses martensite, the amount of martensitic structure is not as much as water-cooled sample. So, it can be derived here that the oil-cooling process has the capability to maintain the hardness, toughness, and ductility in the steel by the virtue of imparting ferrite, cementite, and martensite simultaneously. Figures 8(f) and 8(g) show the microstructures of air-cooled sample. These images are very similar to those of sand-cooled samples. Mainly, pearlite was

observed in a clear lamellar form. Air cooling provided the sufficient time to cementite to precipitate over ferrite. Due to this type of microstructure, air-cooled sample possesses proper amount of ductility with good tensile strength.

4. Conclusions

The effect of heat treatment on mechanical properties (tensile strength, hardness, and toughness) and microstructural behavior of welded joint of AISI-1020 samples was analysed in this study. Four different welded plates were heat treated in four different manners. Heating was done up to a common temperature of 1040°C but cooling media were sand, water, oil, and atmospheric air. The following conclusions are made:

- (1) The heat treatment process has made the air-cooled and sand-cooled samples ductile and tough. Both the samples possess high extension values and therefore high strain energy. In addition, the tensile stress of sand-cooled specimen (332 MPa) was found to be 66% higher than that of air-cooled specimen. Also, the extension in sand-cooled specimen is 81% higher than air-cooled specimen. It shows that sand-cooling method has drastically increased the ductile nature of the steel. On the other hand, water-cooled and oil-cooled samples have shown short extension prior to fracture and hence lack of ductility.
- (2) The water-cooled specimen showed the tensile stress of 289 MPa and that is 44% higher than air-cooled specimen but 13% lower than sand-cooled specimen. This tensile strength was achieved with the loss of ductility as the extension was reported very low, i.e., 0.2 mm.
- (3) Oil-cooled specimen showed a good combination of strength and ductility. It showed the highest tensile stress of 550 MPa which is 175%, 90%, and 65% higher than that of air-cooled, water-quenched, and sand-cooled specimens, respectively. Also, it possessed 146% higher extension than water-cooled sample. It indicates that the limitations involved in the water-cooling method can be overcome by the oil-cooling process.
- (4) Although the hardness profile of all the samples is similar in nature, water-cooled samples showed higher hardness at every point. It can be concluded that hardness at the welded zone > hardness at the heat-affected zone > hardness at the base metal zone.
- (5) The impact test results corroborate with the microstructure. It was found that sand-cooled sample (102 J) possessed the highest toughness among all. Due to martensite formation, water-cooled sample showed only 88 J of toughness.
- (6) The various heat treatment approach has changed the appearance of microstructural appearance of steel. The sand-cooled sample imparts a lamellar-shaped coarse-grained pearlite. Means, austenite has fully converted into pearlite which makes the steel

ductile and tough. The air-cooled sample showed almost similar characteristics of microstructure. However, the exact size of the grains could not be reported in this study. On the other side, the martensitic structure has been observed in water-cooled sample. Oil-cooled sample showed all the three types of microstructures, i.e., ferrite, cementite, and martensite. The bright and dark appearance establish the appearance of ferrite and cementite, respectively. Some needle-like shapes are account of martensitic structure. Therefore, oil-cooled specimen carries an ideal combination of ultimate tensile strength, hardness, toughness, and ductility [23–26].

Data Availability

All data are included within the article.

Conflicts of Interest

The authors declare no conflicts of interest.

References

- [1] S. Dewangan, M. R. Patel, R. Singh, A. Kumar, D. K. Gope, and U. Kumar, "Temperature distribution analysis and hardness measurement into TIG welded stainless steel plates," *AIP Conference Proceedings*, vol. 2148, no. 1, Article ID 30043, 2019.
- [2] S. Dewangan, S. Behera, and M. K. Chowrasia, "Comparative analysis into mechanical properties and microstructural attributes of quenched and tempered 0.2%-C steel," *World Journal of Engineering*, vol. 17, no. 1, pp. 127–133, 2020.
- [3] S. Dewangan, N. Mainwal, M. Khandelwal, and P. S. Jadhav, "Performance analysis of heat treated AISI 1020 steel samples on the basis of various destructive mechanical testing and microstructural behaviour," *Australian Journal of Mechanical Engineering*, vol. 20, no. 1, pp. 74–87, 2022.
- [4] A. G. Olabi and M. S. J. Hashmi, "Stress relief procedures for low carbon steel (1020) welded components," *Journal of Materials Processing Technology*, vol. 56, no. 1-4, pp. 552–562, 1996.
- [5] S. Dewangan, S. K. Mohapatra, and A. Sharma, "An assessment into mechanical properties and microstructural behavior of TIG welded Ti-6Al-4V titanium alloy," *Grey Systems: Theory and Application*, vol. 10, no. 3, pp. 281–292, 2020.
- [6] W. D. Callister, *An Introduction to Materials Science and Engineering*, John Wiley & Sons, New York, NY, USA, 2007.
- [7] "Heat Treatment of welded joints," 2022, <https://www.twi-global.com/technical-knowledge/job-knowledge/heat-treatment-of-welded-joints-part-1-114>.
- [8] N. Yamaguchi, G. Lemoine, T. Shiozaki, and Y. Tamai, "Effect of microstructures on notch fatigue properties in ultra-high strength steel sheet welded joint," *International Journal of Fatigue*, vol. 129, Article ID 105233, 2019.
- [9] L. D. J. Jorge, V. S. Cândido, A. C. R. D. Silva et al., "Mechanical properties and microstructure of SMAW welded and thermally treated HSLA-80 steel," *Journal of Materials Research and Technology*, vol. 7, no. 4, pp. 598–605, 2018.
- [10] F. Deirmina, N. Peghini, B. AlMangour, D. Grzesiak, and M. Pellizzari, "Heat treatment and properties of a hot work

- tool steel fabricated by additive manufacturing,” *Materials Science and Engineering*, vol. 753, pp. 109–121, 2019.
- [11] F. Peng, Y. Xu, D. T. Han, X. Gu, J. Li, and X. Wang, “Influence of pre-tempering treatment on microstructure and mechanical properties in quenching and partitioning steels with ferrite-martensite start structure,” *Materials Science and Engineering*, vol. 756, pp. 248–257, 2019.
- [12] Y. X. Wu, W. W. Sun, M. J. Styles, A. Arlazarov, and C. R. Hutchinson, “Cementite coarsening during the tempering of Fe-C-Mn martensite,” *Acta Materialia*, vol. 159, pp. 209–224, 2018.
- [13] J. Hidalgo, K. O. Findley, and M. J. Santofimia, “Thermal and mechanical stability of retained austenite surrounded by martensite with different degrees of tempering,” *Materials Science and Engineering*, vol. 690, pp. 337–347, 2017.
- [14] Z. H. Guo, F. R. Xiao, S. I. Lu, H. Y. Li, and B. Liao, “Effects of heat-treatment on the microstructure and wear resistance of a high-chromium cast iron for rolls,” *Advances in Materials Science and Engineering*, vol. 2016, Article ID 9807685, 7 pages, 2016.
- [15] A. Çalik, “Effect of cooling rate on hardness and microstructure of AISI 1020, AISI 1040 and AISI 1060 Steels,” *International Journal of the Physical Sciences*, vol. 4, no. 9, pp. 514–518, 2009.
- [16] M. S. Htun, S. T. Kyaw, and K. T. Lwin, “Effect of heat treatment on microstructures and mechanical properties of spring steel,” *Journal of Metals, Materials and Minerals*, vol. 18, pp. 191–197, 2008.
- [17] I. F. Machado, “Technological advances in steels heat treatment,” *Journal of Materials Processing Technology*, vol. 172, no. 2, pp. 169–173, 2006.
- [18] S. S. Kumaran and S. Muthukumaran, “Effect of projection on joint properties of friction welding of tube-to-tube plate using an external tool,” *International Journal of Advanced Manufacturing Technology*, vol. 75, no. 9-12, pp. 1723–1733, 2014.
- [19] S. Sivakumar, S. Senthil Kumaran, M. Uthayakumar, and A. Daniel Das, “Garnet and Al-flyash composite under dry sliding conditions,” *Journal of Composite Materials*, vol. 52, no. 17, pp. 2281–2288, 2018.
- [20] S. K. Selvaraj, K. Srinivasan, M. Ponmariappan, S. Yashwanth, Y. C. Akshay, and Y. C. Hu, “Study of raw and chemically treated *Sansevieria ehrenbergii* fibers for brake pad application,” *Materials Research Express*, Article ID 55102, 15 pages, 2020.
- [21] ASTM E8M-13, “Standard test methods for tension testing of metallic materials,” 2020, <http://www.galvanizeit.com/uploads/ASTM-E-8-yr-13.pdf>.
- [22] R. Maksuti, “Fractographic analysis of welded joint surfaces,” *International Scientific Journal Machines. Technologies. Materials*, vol. 12, pp. 34–37, 2016.
- [23] S. Kannan, S. Senthil Kumaran, and L. A. Kumaraswamidhas, “An investigation on compression strength analysis of commercial Aluminium Tube to Aluminium 2025 Tube Plate by using TIG welding process,” *Journal of Alloys and Compounds*, vol. 666, pp. 131–143, 2016.
- [24] S. Kannan, S. Senthil Kumaran, and L. A. Kumaraswamidhas, “An Investigation on mechanical property of commercial copper tube to Aluminium 2025 tube plate by FWTPET process,” *Journal of Alloys and Compounds*, vol. 672, pp. 674–688, 2016.
- [25] V. R. NazeeraBanu, S. Rajendran, and S. Senthil Kumaran, “Investigation of the inhibitive effect of tween 20 self-assembling nanofilms on corrosion of carbon steel,” *Journal of Alloys and Compounds*, vol. 675, pp. 139–148, 2016.
- [26] S. Senthil Kumaran and A. Daniel Das, “Friction welding joints of SA 213 tube to SA 387 tube plate boiler grade materials by using clearance and interference fit method,” *Materials Today Proceedings*, vol. 5, no. 2, pp. 8557–8566, 2018.